European Journal of Pharmaceutics and Biopharmaceutics 79 (2011) 544–551

Contents lists available at ScienceDirect

European Journal of Pharmaceutics and Biopharmaceutics

journal homepage: www.elsevier.com/locate/ejpb

Research paper

Incorporation of indomethacin nanoparticles into 3-D ordered macroporous silica for enhanced dissolution and reduced gastric irritancy

Yanchen Hu [a], Zhuangzhi Zhi [b], Tianyi Wang [a], Tongying Jiang [a,*], Siling Wang [a,*]

[a] Department of Pharmaceutics, Shenyang Pharmaceutical University, Shenyang, PR China
[b] Department of Physics, Shenyang Pharmaceutical University, Shenyang, PR China

ARTICLE INFO

Article history:
Received 22 November 2010
Accepted in revised form 4 July 2011
Available online 13 July 2011

Keywords:
3-D ordered macroporous silica
Drug nanoparticles
In vitro dissolution
Gastric damage

ABSTRACT

In the present study, we exploited for the first time the potential of 3-D ordered macroporous (3DOM) silica as matrix for drug nanoparticles, in order to obtain proper control over drug particle size in the sub-micrometer range, enhance the dissolution rate, and reduce gastric damage. 3DOM silica matrix with 3-D spherical pores of 200 nm was successfully created and then loaded with IMC nanoparticles at various drug–silica ratios. A rapid release profile for IMC nanoparticle formulations was achieved in comparison with microsized IMC and a commercial capsule, which could be attributed to both increase in the specific surface area and decrease in the crystallinity of IMC, as well as the hydrophilic surface and the interconnected pore networks of 3DOM silica. Reduced gastric damage of IMC was demonstrated, and the protective effect may arise from the reduction in drug particle size as well as encapsulation effect of 3DOM silica.

1. Introduction

Progress in combinatorial chemistry and high throughput screening technology has allowed for the synthesis of an increasing number of new chemical entities (NCE). However, these compounds often show poor aqueous solubility, dissolution-limited absorption, and hence poor and highly variable bioavailability. It is estimated that up to 40% of new chemical entities in development possess insufficient aqueous solubility, which represents a serious challenge for the successful pharmaceutical formulation and marketing [1].

Significant efforts have been done to tackle the formulation challenges of poorly water-soluble drugs, such as micronization, lipid-based formulations, solid dispersion, co-solvents, salt formation, and complexation with cyclodextrin [2–4]. In the last decades, production of nanoparticle has been developed as an alternative approach for the formulation of poorly soluble drugs [5–7]. Typically, nanoparticles consist of pure drug particles and a suitable amount of surface active agents with a mean particle size in the nanometer range, typically between 10 and 1000 nm [8]. According to the Noyes–Whitney and Ostwald–Freundlich equation, reducing particle size within the nanometer range can lead to an increased saturation solubility, enlarged surface area, and an increased dissolution velocity, thus achieving high oral bioavailability [9]. Engineering drug itself in the form of nanoparticles has emerged as a promising strategy for the delivery of poorly soluble drugs. In spite of the progress of the knowledge in this field, nanoparticles have the drawback of instability caused by nucleation and particle growth. In the absence of a stabilizer, the high surface energy of nanosized particles can induce aggregation-a phenomenon known as Ostwald ripening. As a result, a careful and tedious screening of the type and concentration of the stabilizer was usually needed for the production and stabilization of nanoparticles. Also, large quantities of stabilizers, such as polymeric stabilizers and surfactant stabilizers, were usually necessary to ensure adequate stabilization since the total surface area of the nanoparticles was typically orders of magnitude larger compared to a coarse crystal [10]. Hence, it is highly desirable to seek for more effective stabilizer or matrix for nanoparticle formulations.

In the past few years, three dimensionally ordered macroporous (3DOM) materials with pore sizes in the sub-micrometer range have drawn great attention because of their potential applications in catalysis, biosensors, and photonic crystals [11–13]. 3DOM materials are generally synthesized through colloidal crystals template method. The use of colloidal crystal templates, such as close-packed polymer or silica latex spheres, can produce 3DOM materials with spherical pores of typically hundreds of nanometers in diameter. The highly accessible large pores and 3-D interconnected pore networks can reduce the diffusion resistance and permit facile transport, thus allowing ready accessibility to guest molecules and enhanced mass transport [14].

* Corresponding authors. 103 Wenhua Road, Shenyang, Liaoning Province 110016, PR China. Tel./fax: +86 24 23986348.
E-mail addresses: tongyingjiang@yahoo.com.cn (T. Jiang), silingwang@syphu.edu.cn (S. Wang).

0939-6411/$ - see front matter © 2011 Elsevier B.V. All rights reserved.
doi:10.1016/j.ejpb.2011.07.001

With these principles in mind, 3DOM silica possesses several features that render it excellent candidate as matrix for drug nanoparticles. 3DOM silica is chosen in this present study because silica is safe, inert, and a pharmaceutically acceptable inorganic excipient [15,16]. The hypothesis is that if the drug is entrapped completely in the pores, the drug particles should not be larger than the diameter of the silica pores due to the pore dimensional confinement. Drug nanoparticles entrapped into the nanosized pores of 3DOM silica, on the one hand, represent an enlarged specific surface area and, on the other hand, are difficult to form highly ordered crystals due to spatial restrictions, both contributing to an enhanced dissolution rate. Furthermore, the flexible synthesis of colloidal crystals with different sizes allows the easy manipulation of the pore dimensions of 3DOM silica [17], thus ensuring control of drug particle size within sub-micrometers range. Notably, nanoparticles tend to agglomerate automatically because of higher surface energy, which in turn lead to a decrease in dissolution rate. The embedding of drug nanoparticles into honeycomb-like networks of 3DOM silica can prevent them from undergoing agglomeration and growth, thus overcoming this problem.

In light of the above mentions, the goal of the current study was to evaluate the suitability of 3DOM silica as matrix for drug nanoparticles. Furthermore, we wanted to investigate the influence of silica amount on the incorporation and then release properties of drug nanoparticles, aiming to find the optimum drug–silica ratio needed for proper size control and effective nanoparticle incorporation. Indomethacin (IMC), a non-steroidal anti-inflammatory drug, was used as a BCS-2 model drug due to its dissolution-limited absorption [18]. 3DOM silica with pore size of 200 nm was successfully fabricated with PMMA as a template. The solvent deposition method was applied to incorporate IMC nanoparticles into 3DOM silica matrix at various drug–silica ratios (1:1, 1:2 and 1:3). Scanning electron microscopy, powder X-ray diffraction, differential scanning calorimetry, and infrared spectroscopy were used to characterize the corresponding formulation. The release profiles of IMC nanoparticles formulations at different drug–silica ratios were compared, and the possible mechanism for dissolution differences was addressed. Moreover, it was also presumed that the incorporation of IMC nanoparticles into 3DOM silica matrix would produce a protective effect on gastric mucosa compared with the ulcerative effect induced by IMC aqueous suspension.

2. Materials and methods

2.1. Materials

Tetraethoxysilane (TEOS) and methyl methacrylate (MMA) were obtained from Sigma–Aldrich. Indomethacin (purity > 99.0%) and commercial capsule (XIAOYANTONG, 25 mg) were purchased from Shijiazhuang Pharmaceutical Group (Huasheng Pharm. Co., Ltd.). All other chemicals were of analytical/spectroscopic/HPLC grade as required and used as received.

2.2. Fabrication and characterization of 3DOM silica matrix

3DOM silica matrix was prepared using PMMA latex spheres as templates. Non-crosslinked, monodisperse poly-(methyl methacrylate) (PMMA) latex spheres with the diameter of 250 nm were synthesized using an emulsifier-free emulsion polymerization technique described in the literature [19]. Before use, the latex spheres were close-packed into highly ordered colloidal crystal templates by centrifugation for 5 h (3000 rpm) and then allowed to air-dry. The obtained latex spheres were then crushed, and millimeter-thick layers of a suitable amount were deposited on filter paper in a Buchner funnel under vacuum and wetted with ethanol. The silica alkoxide precursor was obtained by diluting 5 ml HCl (0.5 M) in 12 ml deionized water and then mixing with 25 ml TEOS. The mixtures were stirred with a magnetic bar for 15 min, until the temperature dropped to room temperature. The liquid precursor was added dropwise by pipet to cover the latex spheres completely while suction was applied. The resulting products were dried in a vacuum desiccator for 24 h. The latex spheres were then removed by calcinations in air at 580 °C for 6 h, producing white brittle solids.

2.3. Incorporation of drug nanoparticles into 3DOM silica matrix

Drug nanoparticles were incorporated into pores of 3DOM silica matrix through a solvent deposition procedure involving a combination of soaking equilibrium and subsequent rapid solvent evaporation. Prior to drug loading, the solid silica monolith was first crushed gently with a mortar and pestle and then passed through an 80-mesh sieve to obtain fine powders with good flowability. In detail, IMC was dissolved in acetone to obtain a yellow transparent solution (50 mg/ml) and then an aliquot of this solution was mixed with certain amount of 3DOM silica to obtain samples with different drug–silica ratios (1:1, 1:2, and 1:3, w/w). After gentle stirring for 12 h, the solvent was allowed to evaporate under reduced pressure. The residue was placed in a vacuum desiccator with blue silica gel until no organic solvent was detected by thermal analysis. The obtained nanoparticle preparations with different drug–carrier ratios (1:1, 1:2, and 1:3) were labeled as M1-1, M1-2 and M1-3, respectively. Physical mixtures of 3DOM silica and IMC with the same ratios were also prepared and labeled as PM1-1, PM1-2, and PM1-3, respectively.

2.4. Drug content analysis

An accurately weighed quantity of nanoparticle preparation equivalent to 25 mg of IMC was taken and the drug content determined by ultraviolet (UV) spectroscopy at a wavelength of 320 nm (UV-2000, Unico, USA). Methanol was used to completely extract IMC from samples. The mean of three determinations was calculated. All the preparations were within 100 ± 5% of the theoretical value.

2.5. Field emission scanning electron microscopy (FE-SEM)

The morphology of 3DOM silica matrix, crude IMC and drug nanoparticle preparations at various drug–silica ratios was examined by using a field emission scanning electron microscope (JEOL-6700, Japan). Prior to examination, samples were mounted onto metal stubs using double-sided adhesive tape and sputtered with a thin layer of gold under vacuum.

2.6. Solid state characterization

The solid state of IMC in 3DOM silica matrix was evaluated by differential scanning calorimetry (DSC) and powder X-ray diffractometry (PXRD). DSC was performed on a differential scanning calorimeter (DSC 60, Shimadzu Co., Japan). The equipment was calibrated using indium and zinc. Samples were heated at 10 °C/min in aluminum pans under a nitrogen flow. PXRD was performed using a Rigaku Geigerflex powder X-ray diffractometer (Rigaku Denki, Japan) with a copper anode (Cu Kα radiation, λ = 0.15405 nm, 30 kV, 30 mA). XRD patterns were recorded over the 2θ range from 5° to 50° with a step size of 0.02° and a scan speed of 4°/min. The crystallite size was calculated from the width of the characteristic line at 2θ = 11.7° using the Scherrer equation corrected for instrumental broadening.

2.7. Fourier transform infrared spectroscopy (FT-IR spectroscopy)

Infrared spectra of the samples were obtained using a FT-IR spectrometer (Bruker, IFS 55, Switzerland). Samples were milled and mixed with 100-fold amount of dried KBr in an agate mortar and pestle. KBr disks were prepared with a compression force of 10 tons using a 13-mm-diameter round flat face punch. Infrared spectra were recorded from 400 to 4000 cm^{-1} in transmittance mode, with a resolution of 1 cm^{-1}.

2.8. In vitro dissolution testing

Dissolution tests were carried out with USP dissolution apparatus using the paddle method (KC-8D, Tianjin Guoming Medical Equipment Co. Ltd.). The dissolution medium consisted of 900 ml phosphate buffer (pH 6.8) prepared using KH_2PO_4 and NaOH. Dissolution studies were carried out at 37 ± 0.5 °C with a paddle speed of 100 ± 1 rpm. A sample corresponding to 25 mg IMC was introduced onto the surface of dissolution medium at zero time. Aliquots (5 ml) of the dissolution medium were withdrawn and passed through a 0.45-μm membrane filter at appropriate intervals (5, 10, 15, 20, 30, 45, and 60 min). A UV detection wavelength of 320 nm was used to determine the amount of IMC dissolved. All measurements were carried out in triplicate.

2.9. Gastric mucosa irritation test

All experimental procedures carried out in this study were performed in accordance with the Guidelines for the Care and Use of Laboratory Animals of Shenyang Pharmaceutical University. Fifteen rats, weighing 250 ± 20 g, were divided into three groups. After 20 h of fasting, one group was orally gavaged with normal saline as control, while the other two groups were given by oral gavage pure IMC powders and the M1-3 preparations at a single dose of 20 mg IMC/kg (suspended in aqueous suspension of normal saline). Five hours after administration, all rats were sacrificed, with stomach removed and rinsed thoroughly with physiological saline. Later, the stomachs were opened along the line of greater curvature from the duodenum to the pyloric sphincter and then spread flat and examined for damage macroscopically. The damage score (DS) was assessed [20] based on the severity of mucosa injury on a 0–4 scale: 0 – almost normal mucosa, 0.5 – hyperemia, 1 – one or two lesions, 2 – severe lesions, 3 – very severe lesions, and 4 – mucosa full of lesions (lesions-hemorrhagic erosions, hyperemia-vascular congestions). The sum of the total scores divided by the number of animals was expressed as the mean damage score (ulcer index). Afterward, the lesion part was sectioned for histological studies. The tissue samples were fixed in 10% formalin and embedded in paraffin. The sections (5 μm) were cut using a microtome and stained with hematoxylin and eosin before light microscopic evaluation.

3. Results and discussion

3.1. Preparation and characterization of 3DOM silica carrier

In the present experiment, 3DOM silica was constructed by colloidal crystal template method. Polymer latex spheres (e.g., PAMAM and PS spheres) and silica beads have been the most commonly used colloidal crystal templates for 3DOM materials. One major advantage of this method was that the pore dimensions of 3DOM materials could be easily controlled, depending on the size of the colloidal crystals [21]. Approaches, such as soap-free emulsion polymerization and dispersion polymerization, can be selectively employed to synthesize latex beads with desired particle sizes ranging from l00 nm to more than 1 μm [17]. In this work, PMMA latex spheres with a narrow size distribution were obtained by soap-free emulsion polymerization. Close-packed arrays of latex spheres were formed upon centrifugation. The average particle size and morphology of the latex spheres were characterized by scanning electron microscopy. Fig. 1A presented typical SEM images of PMMA nanospheres in a dry monolithic form. It was found that PMMA colloidal spheres were closely packed into a highly ordered three-dimensional arrangement with uniform particle size of 250 nm. This obtained well-arranged three-dimensional colloidal crystal arrays could be available templates for the creation of 3DOM silica materials. Fig. 1B showed the image of 3DOM silica with PMMA spheres as colloidal crystal templates. The image revealed the formation of well-defined 3-D ordered macroporous structures. The spherical macropores were interconnected through windows that were formed as a result of the contact between the template spheres prior to infiltration of the precursor solution. The pore size was estimated to be approximately 200 nm, estimated by scanning electron microscopy. In comparison with the original colloidal spheres, the pore sizes were slightly reduced due to calcinations shrinkage.

Originally, the obtained 3DOM silica was a solid monolith. Therefore, milling and sieving were desirable in order to produce uniform particles. To investigate whether mechanical processing could destroy the porous structure of 3DOM silica, SEM images of 3DOM silica were obtained after milling. Fig. 1C showed that the pore structure of 3DOM silica did not break and remained intact after grinding. The above investigation shows that it was possible and simple to prepare 3DOM silica particles suitable as a carrier for poorly soluble drugs.

3.2. Drug nanoparticle incorporation into 3DOM matrix

In this experiment, solvent deposition method was applied to load IMC nanoparticle into pores of 3DOM silica (Fig. 2). In principle, the rapid solvent evaporation in the matrix-suspended solution leads to fast nucleus formation of drugs in the nanopores of 3DOM silica matrix. Due to the pore restrictions, the extent of particle growth could be decreased and furthermore the particle size controlled. As shown in Fig. 3A, crude IMC powder was found to be irregular-shaped particles with a relatively wide particle size distribution (mean particle size of several micrometers). However, after incorporation into 3DOM silica by the solvent deposition method, large crystals of IMC disappeared and the outer pores of 3DOM silica were blocked and became ambiguous, suggesting the successful entrapment of IMC into 3DOM silica. Specially, traces of needle-like crystals with several hundred nanometers in size could be observed on the surface of M1-1, M1-2, and M1-3 formulations. Furthermore, with the increase in the silica amount, drug crystals on the outer surface became few and negligible, such as M1-3 formulation with highest silica amount. However, drug crystals were obvious for nanoparticle formulation with drug–silica ratio of 1:1, which might be due to that the drug amount exceeded the pore volume capacity of 3DOM silica. Therefore, we concluded that sufficient silica amount was a prerequisite for the fine dispersion and complete incorporation of drugs.

It is worth noting that the pore size of 3DOM silica can be tailored depending on the diameter of the colloidal crystal; hence, it is speculated that the drug crystals confined inside the pores of 3DOM materials might have the same size with the pores, allowing for the proper control of drug particle size. Engineering drug itself in the form of nanoparticles has emerged as a promising strategy for the delivery of poorly soluble drugs. By applying a variety of loading methods, such as melting adsorption, solvent method, anti-solvent precipitation, and the supercritical carbon dioxide

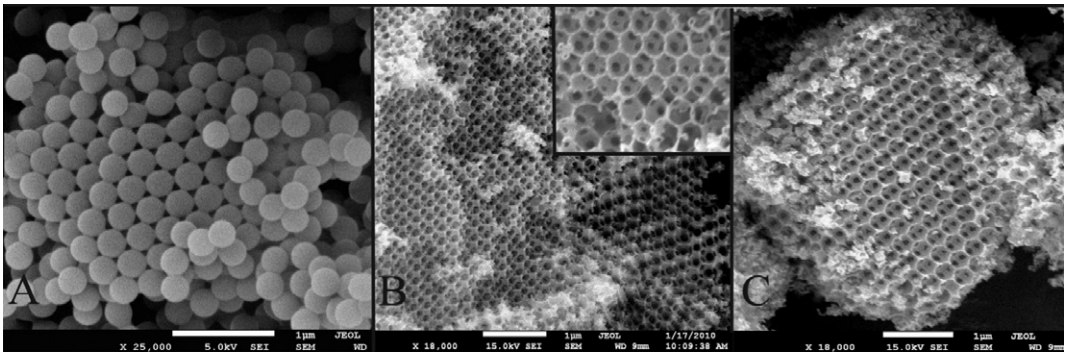

Fig. 1. SEM images of (A) PMMA template (B) 3DOM silica matrix, (C) 3DOM silica remaining its intact porous structure after mechanical processing. Scale bar = 1 micrometer.

Fig. 2. Schematic representation for incorporation of IMC nanoparticles into 3DOM silica matrix. By solvent deposition method, the original large crystals of IMC can be successfully entrapped into pores of 3DOM silica in the form of nanoparticles, thus allowing for the proper size control of drug particle size. (For interpretation of the references to color in this figure legend, the reader is referred to the web version of this article.)

method, it is anticipated that drug particles can be entrapped successfully into the pores of 3DOM silica. Thakur et al. [15] employed porous silica as a carrier or spacer for the precipitated drug particles in order to not only improve the flowability but also obtain a proper particle size control. They demonstrated that the used porous silica could give drug particles an area to adhere to, by either becoming entrapped in the pores or adsorbed on the surface to avoid particle agglomeration.

3.3. Solid state characterization by PXRD and DSC

The crystal property of pure IMC, 3DOM silica, physical mixtures of IMC and silica, and corresponding nanoparticle formulations at various drug–silica ratios was evaluated by PXRD analysis. As shown in the PXRD patterns (Fig. 4), pure IMC showed intense and characteristic diffraction peaks at $2\theta = 11.7°$, 17.0°, 19.8°, 22.0°, and 26.8°, which corresponded to the stable γ-form of IMC. However, 3DOM silica did not show any diffraction peak due to its amorphous nature. For physical mixtures of IMC and silica, the characteristic diffraction peaks of IMC still remained. However, after incorporation into 3DOM silica, a significant loss of IMC crystallinity was observed, irrespective of drug–silica ratios. Furthermore, the intensity markedly decreased with increased amounts of silica. In the case of M1-3 formulation at drug–silica ratio of 1:3, only very weak peaks could be detected, suggesting the lowest degree of crystallinity. The crystalline size of M1-1, M1-2, and M1-3 preparation, calculated by Jade 5.0 software, was reduced to 10.4 nm, 8.8 nm, and 7.0 nm from the initial 42.4 nm of the pure IMC crystals.

Further confirmation of the crystal properties was achieved by evaluation of the thermal behavior using DSC. DSC is a sensitive and powerful tool in recognition of small crystals, where a melting temperature depression can be observed for small nanoparticles. Fig. 5 showed the DSC thermograms of pure IMC, 3DOM silica, physical mixtures of IMC and silica, and corresponding nanoparticle formulations at various drug–silica ratios. For both the crystalline IMC and the physical mixtures, a single sharp endothermic melting peak at 161 °C was observed, in agreement with the melting point of γ-crystalline IMC. However, when loaded into 3DOM silica, IMC suffered a marked reduction in crystallinity reflected in the decreased AUC of the melting peak at 161 °C. In the case of IMC-loaded formulation at a ratio of 1:3, IMC displayed the greatest reduction in crystallinity, with no trace of an endothermic peak at 161 °C observed in the DSC curves. In combination with PXRD analysis, we concluded that only traces of crystalline IMC were present in the M-3 formulation. This observed loss of endothermic peak could be ascribed to that the amount of crystalline IMC was too small to detect due to insufficient sensitivity of the DSC instrument. In particular, in the DSC curves of IMC nanoparticles formulations, there appeared a wide endothermic peak at around 90 °C, an exothermic peak at 108 °C, and an endothermic peak at 155 °C. The endothermic peak at about 90 °C was attributed to the evaporation of physically adsorbed water, while the later two peaks demonstrated the presence of amorphous IMC in nanoparticle preparations [22]. The exothermic peak at 108 °C was associated with the crystallization of amorphous IMC, and the melting peak at 155 °C corresponding to the meta-stable α-form was attributed to a thermodynamic transition from amorphous to meta-stable crystalline IMC during the heating process in the DSC operation. The observed amorphous IMC could be attributed to the space confinement or the hydrogen bonding, which took place between the silanol groups present on the surface of silica and carboxyl group in IMC. Hydrogen bonding between different compounds and porous adsorbents has been reported in the literature as one reason for the observed loss of crystallinity [23,24].

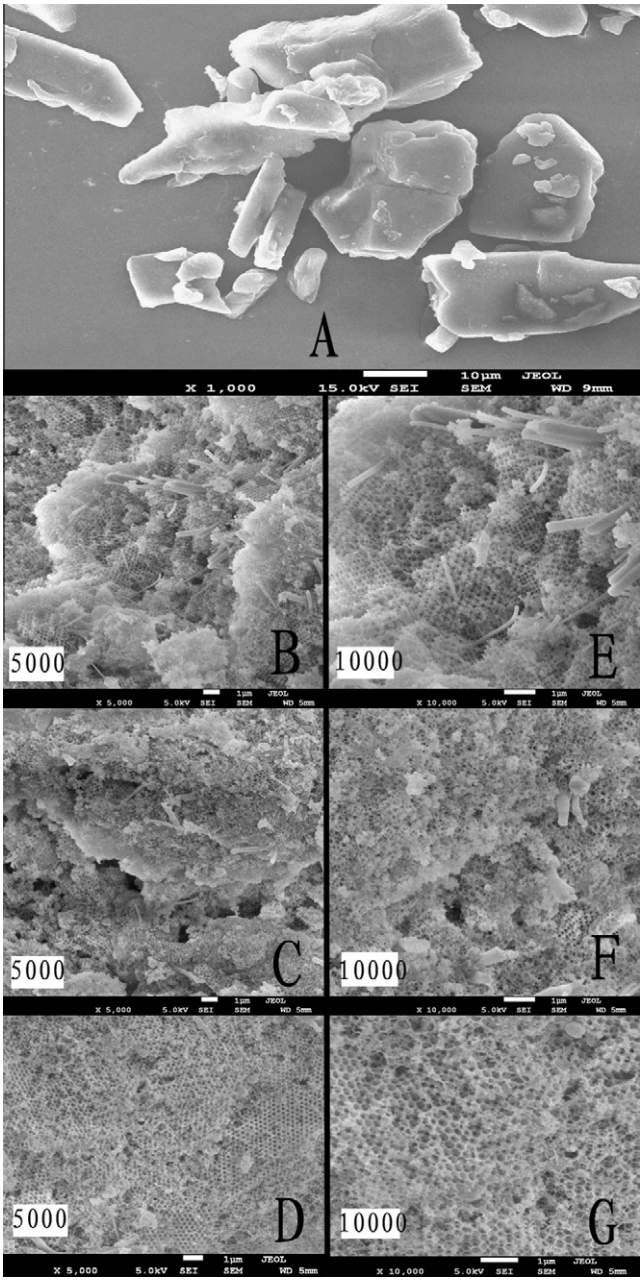

Fig. 3. SEM images of (A) pure IMC powder, (B) M1-1 preparation (×5000), (C) M1-2 preparation (×5000), and (D) M1-3 preparation (×5000). (E) M1-1 preparation (×10,000), (F) M1-2 preparation (×10,000), and (G) M1-3 preparation (×10,000). Scale bar = 1 micrometer.

3.4. FT-IR analysis

To get a better understanding of the solid state of IMC, the IR spectra were used to examine possible intermolecular interactions between IMC and silica matrix. The IR spectra for pure IMC, 3DOM silica, IMC-loaded 3DOM silica formulations, and the corresponding physical mixtures were presented in Fig. 6, and the wave-number region of 800–1800 cm^{-1} was taken and enlarged. Pure IMC showed its characteristic peaks at 1716 and 1691 cm^{-1} (corresponding to the carbonyl group of the acid and amide, respectively). In contrast, in the IR spectrum of the IMC-loaded 3DOM silica formulation, the originally strong carbonyl stretching peaks were weaker and broader and shifted to lower wavenumbers of 1705 cm^{-1} and 1679 cm^{-1}, corresponding to the acid and amide

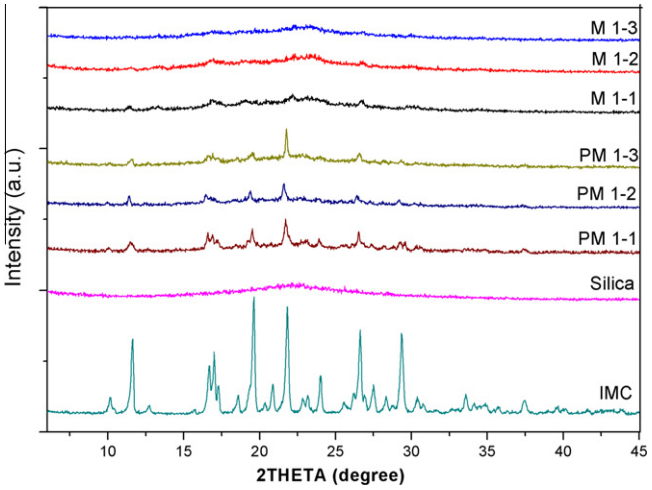

Fig. 4. XRD patterns for pure IMC, 3DOM silica, physical mixtures, and corresponding nanoparticle preparations. (For interpretation of the references to color in this figure legend, the reader is referred to the web version of this article.)

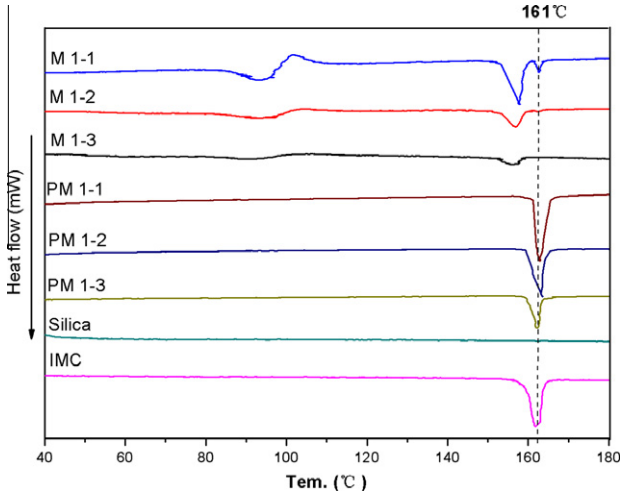

Fig. 5. DSC thermograms for pure IMC, 3DOM silica, physical mixture, and corresponding nanoparticle preparations. (For interpretation of the references to color in this figure legend, the reader is referred to the web version of this article.)

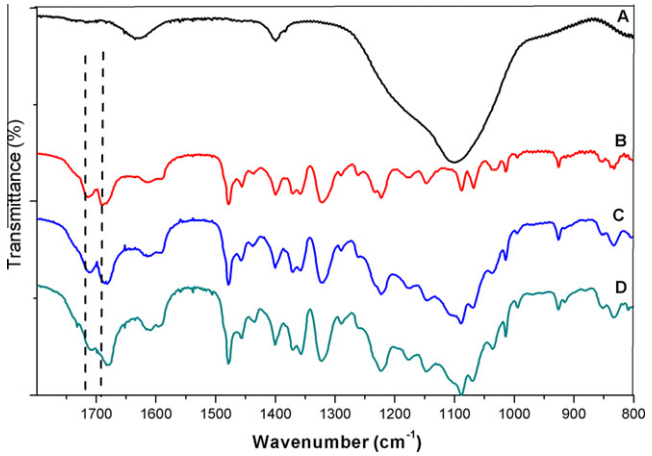

Fig. 6. FT-IR spectra of (A) 3DOM silica, (B) pure IMC, (C) physical mixture of IMC and 3DOM silica, (D) M1-3 preparation. (For interpretation of the references to color in this figure legend, the reader is referred to the web version of this article.)

groups, respectively. This shift indicated that the acid and amide functional groups were involved in hydrogen bonding with the silica surface. The hydrogen bond formed in the physical mixtures might be attributed to the simple blending or the KBr disk sampling process, which involved the grinding of IMC and silica. Intermolecular interaction has been reported to form by physical mixing of silica with IMC [25]. Various reports have been published on the interactions between IMC molecules and silica, wherein the silanol group on the surface of silica particles tends to form hydrogen bonds with the carbonyl group of the drug [26,27]. Furthermore, the hydrogen bonding between drug molecules and silica has proved to facilitate the stabilizing of the amorphous form of drugs [28].

3.5. In vitro dissolution

In the present work, the release profile of IMC nanoparticle formulations at various drug–silica ratios was measured and compared with those of the corresponding physical mixtures as well as original IMC crystals and a commercial capsule. As presented in Fig. 7, for pure IMC crystals, 60% of IMC dissolved within 60 min, indicating the poor dissolution of the pure drug. The physical mixtures of 3DOM silica and IMC (PM1-1, PM1-2, and PM1-3) exhibited almost the same dissolution profiles with that of pure IMC. However, the dissolution of IMC from all the IMC nanoparticle formulations, irrespective of drug-to-silica ratio, was significantly higher than that from pure IMC, the commercial capsule, and the physical mixtures. Furthermore, the release profiles for nanoparticles formulations with different drug–silica ratios were compared in order to investigate the effect of silica amount on dissolution behavior of IMC and to optimize drug–carrier ratios for dosage. As depicted in Fig. 7, on increasing the amount of silica, the dissolution rate of IMC increased. The formulation with the highest silica content (drug–silica ratio = 1:3) exhibited the fastest dissolution rate, with more than 80% dissolved within 5 min. This may be ascribed to the improved dispersibility and wettability as well as the extremely low content of crystalline form present in M1-3 formulations.

Several factors may contribute to the dissolution enhancement: the lack of crystalline form and presence of amorphous form, the reduction in drug particle size to nanosize range and the hydrophilic surface as well as the interconnected pore networks of 3DOM silica. Nanoparticle or nanosizing technique has been considered as an effective way to increase the dissolution velocity, because nanosized drug crystals could increase the effective surface area available for dissolution. Besides, since the pore size of 3DOM silica was controlled in the hundred nanometers range, the formation of the highly ordered crystalline IMC is restricted by the confined space of the pores, thus retaining in its non-crystalline or amorphous form. The formation of the less ordered or amorphous form, compared with the crystalline form, is well known to dramatically increase the apparent solubility and dissolution rate of poorly water-soluble drugs [25]. In addition, the hydrophilic surface and interconnected pore networks of 3DOM silica could facilitate the wettability and facile transport of poorly soluble drugs, resulting in a fast dissolution.

Mesoporous silica (2 nm < pore size < 30 nm) has been widely used to encapsulate poorly soluble drugs in order to obtain fast drug release, such as MCM-41 [29], TUD [30], and SBA-15 [31]. The improvement of dissolution rate was ascribed to the lack of drug in the crystalline form and the extremely large surface area of porous silica. In contrast to ordered mesoporous silica templated by surfactant micelles, 3DOM silica was templated by colloidal crystals, allowing the introduction of larger pores with controlled size, typically hundreds of nanometers in diameter. It was speculated that the large pore size and highly accessible surface areas might be more advantageous for drug nanoparticles introduction and then rapid drug release.

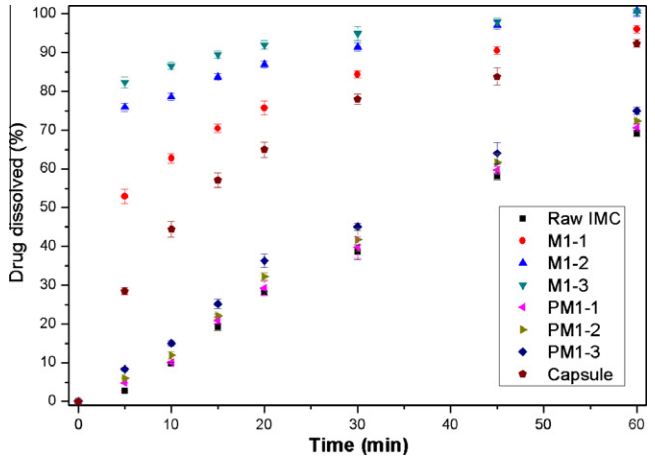

Fig. 7. In vitro dissolution profiles of pure IMC powders, the commercial capsule, the physical mixtures of 3DOM silica and IMC (PM 1-1, PM 1-2, and PM 1-3), and corresponding nanoparticle preparations (M1-1, M1-2, and M1-3). (For interpretation of the references to color in this figure legend, the reader is referred to the web version of this article.)

3.6. Gastric mucosa irritation test

Indomethacin, a non-steroidal anti-inflammatory drug (NSAID) with analgesic and anti-pyretic properties, has been widely used to reduce inflammation and pain. However, its efficacy is often offset due to the poor aqueous solubility and the incidence of gastrointestinal ulceration and hemorrhage. In our recent report, an indomethacin-5-fluorouracil-methyl ester dry emulsion was prepared in order to produce a combined effect of IMC and 5-fluorouracil for cancer therapy as well as to reduce the side effects of IMC [32].

In this work, it was anticipated that incorporation of IMC nanoparticles into 3DOM silica can produce a protective effect on the gastric mucosa compared with the ulcerative effect caused by IMC aqueous suspension. Noticeable hemorrhagic damage was observed on the mucosal surface when IMC solution was administered to rats. In contrast, only hyperemia and pinpointed lesions were apparent following oral administration of IMC nanoparticle formulation (Fig. 8). The protective effect was further conformed by histological analysis. Mucosal bleeding and inflammatory cell infiltrations developed in rats after administration of IMC aqueous solution while administration of IMC nanoparticle formulations

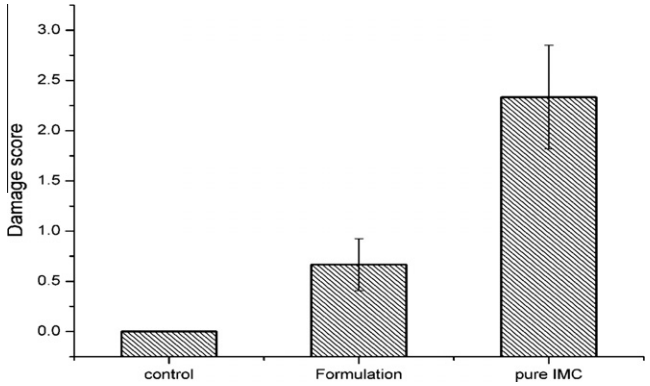

Fig. 8. Gastric damage scores following oral administration of IMC (20 mg/kg) to rats ($n = 5$).

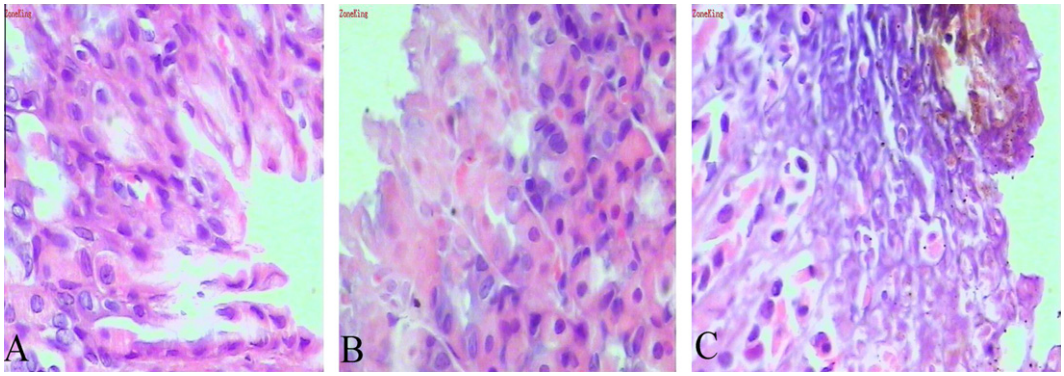

Fig. 9. Histological examination for mucosal damage of rats following oral administration of (A) normal saline, (B) M1-3 preparation, (C) IMC aqueous solution. (For interpretation of the references to color in this figure legend, the reader is referred to the web version of this article.)

significantly inhibited these changes (Fig. 9). Liversidge and Conzentino demonstrated that a drug particle size reduction (from 20 μm to 270 nm) could reduce gastric irritation and enhance the absorption of naproxen in rats following oral administration. The reduced irritation was attributed to a decrease in the local high and prolonged concentration of drugs since there was no longer large crystal in contact with the mucosa [33]. In addition, there have been reports that the encapsulation of IMC into nanocapsule formulations could protect gastrointestinal mucosa from ulceration, probably by avoiding direct contact of free drugs with the surface of mucosa [34]. Therefore, in our present study, it appeared that the reduced irritation arose from both the reduction in drug particle size and protective effect of 3DOM silica matrix.

4. Conclusions

The effective inclusion and then rapid release of IMC nanoparticles was reported in our present study. Investigations using SEM, XRD, DSC, and IR demonstrated the successful entrapment of IMC nanoparticles into the 3DOM silica and the existing interactions between drug guest molecule and silica host. A significant loss of crystallinity and partial crystalline-amorphous transformation were observed for IMC after incorporation into 3DOM silica. The significant crystallinity reduction was probably due to spatial confinement and hydrogen bonds formation between silica and IMC. It was showed that IMC nanoparticle formulations exhibited a marked promotion of in vitro dissolution rate. Several factors seemed to play roles for the dissolution enhancement effect, including the lack of crystalline form and presence of amorphous form, particle size reduction to the nanosize range, and the hydrophilic surface as well as the interconnected pore networks of 3DOM silica. As a result of these facts, 3DOM silica is likely to be an excellent candidate for the oral delivery of water-insoluble drugs, such as IMC, to obtain proper size control, enhanced dissolution rate, and reduced gastric mucosa irritation.

We believe that the effective delivery of IMC by 3DOM silica will, on the one hand, open up a new application field for 3DOM materials and, on the other hand, provide a new strategy to formulate poorly soluble drugs.

Acknowledgements

This work was financially supported by National Basic Research Program of China (973 Program) (No. 2009CB930300), National Natural Science Foundation of China (No. 81072605), Major National Platform for Innovative Pharmaceuticals (2009ZX09301-012) and Key Laboratory of Drug Preparation Design & Evaluation of Liaoning Provincial Education Department. In particular, we thank Dr. David for languages correction.

References

[1] C.A. Lipinski, F. Lombardo, B.W. Dominy, P.J. Feeney, Experimental and computational approaches to estimate solubility and permeability in drug discovery and development settings, Adv. Drug Deliv. Rev. 46 (2001) 3–26.
[2] M. Vogt, K. Kunath, J.B. Dressman, Dissolution enhancement of fenofibrate by micronization, cogrinding and spray-drying: comparison with commercial preparations, Eur. J. Pharm. Biopharm. 68 (2008) 283–288.
[3] D.J. Hauss, Oral lipid-based formulations, Adv. Drug Deliv. Rev 59 (2007) 667–676.
[4] J. Dressman, C. Reppas, Drug solubility: how to measure it, how to improve it, Adv. Drug Deliv. Rev 59 (2007) 531–532.
[5] C. Keck, R. Muller, Drug nanocrystals of poorly soluble drugs produced by high pressure homogenisation, Eur. J. Pharm. Biopharm. 62 (2006) 3–16.
[6] R.H. Müller, C. Jacobs, O. Kayser, Nanosuspensions as particulate drug formulations in therapy: rationale for development and what we can expect for the future, Adv. Drug. Deliv. Rev 47 (2001) 3–19.
[7] E. Merisko-Liversidge, G.G. Liversidge, E.R. Cooper, Nanosizing: a formulation approach for poorly-water-soluble compounds, Eur. J. Pharm. Sci 18 (2003) 113–120.
[8] L. Gao, D. Zhang, M. Chen, Drug nanocrystals for the formulation of poorly soluble drugs and its application as a potential drug delivery system, J. Nanopart. Res. 10 (2008) 845–862.
[9] F. Kesisoglou, S. Panmai, Y. Wu, Nanosizing – oral formulation development and biopharmaceutical evaluation, Adv. Drug Deliv. Rev. 59 (2007) 631–644.
[10] B. Van Eerdenbrugh, G. Van den Mooter, P. Augustijns, Top-down production of drug nanocrystals: nanosuspension stabilization, miniaturization and transformation into solid products, Int. J. Pharm. 364 (2008) 64–75.
[11] J. Liu, Y. Cai, Y. Deng, Z. Sun, D. Gu, B. Tu, D. Zhao, Magnetic 3-D ordered macroporous silica templated from binary colloidal crystals and its application for effective removal of microcystin, Micropor. Mesopor. Mater 130 (2010) 26–31.
[12] H.Y.JustinC. Lytle, Nicholas S. Ergang, William H. Smyrl, Andreas Stein, Structural and electrochemical properties of three-dimensionally ordered macroporous tin(IV) oxide films, J. Mater. Chem. 14 (2004) 1616–1622.
[13] F. Su, X. Zhao, Y. Wang, J. Zeng, Z. Zhou, J. Lee, Synthesis of graphitic ordered macroporous carbon with a three-dimensional interconnected pore structure for electrochemical applications, J. Phys. Chem. B 109 (2005) 20200–20206.
[14] K. Lee, J. Lytle, N. Ergang, S. Oh, A. Stein, Synthesis and rate performance of monolithic macroporous carbon electrodes for lithium–ion secondary batteries, Adv. Funct. Mater 15 (2005) 547–556.
[15] R. Thakur, A. Hudgins, E. Goncalves, G. Muhrer, Particle size and bulk powder flow control by supercritical antisolvent precipitation, Ind. Eng. Chem. Res. 48 (2009) 5302–5309.
[16] H. Friedrich, B. Fussnegger, K. Kolter, R. Bodmeier, Dissolution rate improvement of poorly water-soluble drugs obtained by adsorbing solutions of drugs in hydrophilic solvents onto high surface area carriers, Eur. J. Pharm. Biopharm. 62 (2006) 171–177.
[17] J. Zhang, Y. Jin, C. Li, Y. Shen, L. Han, Z. Hu, X. Di, Z. Liu, Creation of three-dimensionally ordered macroporous Au/CeO_2 catalysts with controlled pore sizes and their enhanced catalytic performance for formaldehyde oxidation, Appl. Catal. B: Environ. 91 (2009) 11–20.
[18] A. Allahham, P.J. Stewart, Enhancement of the dissolution of indomethacin in interactive mixtures using added fine lactose, Eur. J. Pharm. Biopharm. 67 (2007) 732–742.
[19] D. Zou, S. Ma, R. Guan, M. Park, L. Sun, J. Aklonis, R. Salovey, Model filled polymers. V. Synthesis of crosslinked monodisperse polymethacrylate beads, J. Polym. Sci. Part A: Polym. Chem. 30 (2003) 137–144.

[20] D. Dokmeci, M. Akpolat, N. Aydogdu, L. Doganay, F. Turan, L-carnitine inhibits ethanol-induced gastric mucosal injury in rats, Pharmacol. Rep. 57 (2005) 481–488.
[21] Y. Xia, B. Gates, Y. Yin, Y. Lu, Monodispersed colloidal spheres: old materials with new applications, Adv. Mater. 12 (2000) 693–713.
[22] F. Wang, H. Hui, T. Barnes, C. Barnett, C. Prestidge, Oxidized mesoporous silicon microparticles for improved oral delivery of poorly soluble drugs, Mol. Pharm. 7 (2009) 227–236.
[23] C. Ji, Angela Barrett, Laura A. Poole-Warren, Neil R. Foster, Fariba Dehghani, The development of a dense gas solvent exchange process for the impregnation of pharmaceuticals into porous chitosan, Int. J. Pharm. 391 (2010) 187–196.
[24] S. Madieh, M. Simone, W. Wilson, D. Mehra, L. Augsburger, Investigation of drug-porous adsorbent interactions in drug mixtures with selected porous adsorbents, J. Pharm. Sci. 96 (2007) 851–863.
[25] X. Pan, T. Julian, L. Augsburger, Increasing the dissolution rate of a low-solubility drug through a crystalline–amorphous transition: a case study with indomethicin, Drug Dev. Ind. Pharm. 34 (2008) 221–231.
[26] T. Watanabe, S. Hasegawa, N. Wakiyama, A. Kusai, M. Senna, Comparison between polyvinylpyrrolidone and silica nanoparticles as carriers for indomethacin in a solid state dispersion, Int. J. Pharm. 250 (2003) 283–286.
[27] H. Takeuchi, S. Nagira, H. Yamamoto, Y. Kawashima, Solid dispersion particles of amorphous indomethacin with fine porous silica particles by using spray-drying method, Int. J. Pharm. 293 (2005) 155–164.
[28] T. Watanabe, N. Wakiyama, F. Usui, M. Ikeda, T. Isobe, M. Senna, Stability of amorphous indomethacin compounded with silica, Int. J. Pharm. 226 (2001) 81–91.
[29] V. Ambrogi, L. Perioli, F. Marmottini, S. Giovagnoli, M. Esposito, C. Rossi, Improvement of dissolution rate of piroxicam by inclusion into MCM-41 mesoporous silicate, Eur. J. Pharm. Sci. 32 (2007) 216–222.
[30] T. Heikkilä, J. Salonen, J. Tuura, M.S. Hamdy, G. Mul, N. Kumar, T. Salmi, D.Y. Murzin, L. Laitinen, A.M. Kaukonen, J. Hirvonen, V.P. Lehto, Mesoporous silica material TUD-1 as a drug delivery system, Int. J. Pharm. 331 (2007) 133–138.
[31] R. Mellaerts, R. Mols, J.A.G. Jammaer, C.A. Aerts, P. Annaert, J. Van Humbeeck, G. Van den Mooter, P. Augustijns, J.A. Martens, Increasing the oral bioavailability of the poorly water soluble drug itraconazole with ordered mesoporous silica, Eur. J. Pharm. Biopharm. 69 (2008) 223–230.
[32] J. Wang, Y. Hu, L. Li, T. Jiang, S. Wang, F. Mo, Indomethacin-5-fluorouracil-methyl ester dry emulsion: a potential oral delivery system for 5-fluorouracil, Drug Dev. Ind. Pharm (2010) 647–656.
[33] P.C. Gary, G. Liversidge, Drug particle size reduction for decreasing gastric irritancy and enhancing absorption of naproxen in rats, Int. J. Pharm. (1995) 309–313.
[34] N. Ammoury, H. Fessi, J. Devissaguet, M. Dubrasquet, S. Benita, Jejunal absorption, pharmacological activity, and pharmacokinetic evaluation of indomethacin-loaded poly (D,L-lactide) and poly (isobutyl-cyanoacrylate) nanocapsules in rats, Pharm. Res. 8 (1991) 101–105.